Measurements of laser-speckle-induced perturbations in laser-driven foils

S. G. Glendinning,[1] S. N. Dixit,[1] B. A. Hammel,[1] D. H. Kalantar,[1] M. H. Key,[2,3] J. D. Kilkenny,[1] J. P. Knauer,[4] D. M. Pennington,[1] B. A. Remington,[1] R. J. Wallace,[1] and S. V. Weber[1]

[1]*Lawrence Livermore National Laboratory, University of California, Livermore, California 94550*

[2]*Central Laser Facility, Rutherford Appleton Laboratory, Chilton, Oxon, OX11 0Qk, United Kingdom*

[3]*Clarendon Laboratory, Department of Physics, University of Oxford, Oxford, OX1 3PU, United Kingdom*

[4]*Laboratory for Laser Energetics, 250 East River Road, Rochester, New York 14623*

(Received 14 February 1996)

We have measured modulations imprinted by laser speckle in laser-driven CH_2 foils at 10^{14} W/cm^2 (laser wavelength 0.53 μm). We have calibrated the amplitude and Rayleigh-Taylor growth of these modulations with single-mode surface perturbations, converting the imprint to an equivalent surface finish. We examined this imprint for a static speckle pattern and with two different bandwidths on the drive laser. The addition of bandwidth and dispersion to the drive laser reduced the imprinted modulations, with the highest bandwidth showing the largest reduction in imprint, in agreement with LASNEX simulations. [S1063-651X(96)06309-X]

PACS number(s): 52.50.Jm, 52.35.Py, 52.65.−y

Growth of modulations in an inertially confined fusion (ICF) capsule, whether initially due to capsule surface finish or drive nonuniformity, may fatally disrupt an ICF implosion by causing cold shell material to mix into the fuel [1,2]. When a capsule is driven by x rays produced inside a hohlraum, the dominant modulations are seeded by the capsule surface finish. When laser light directly drives the capsule the modulations in the driver may be significant. Recent experiments [3,4] have reported reductions in imprint using smoothed laser beams, i.e., laser beams that have a reduced level of spatial nonuniformities. Another technique for reducing imprint has been the use of foams with gold layers [5,6]. In this paper, we report measurements that quantified the equivalence between laser imprinted modulations and surface perturbation.

In our experiment we used laser ablation to accelerate 20-μm-thick CH_2 foils with one arm of the Nova laser at 0.53 μm wavelength. This arm was smoothed with a random phase plate (RPP) [7] and spectral dispersion [8] (SSD), with three different bandwidths in separate experiments: 0.003 THz (the intrinsic bandwidth, introduced by the pulse shaping system), 0.6 THz, and 0.9 THz. A diffraction grating gave 0.086 μrad/THz dispersion and a temporal skew of 110 ps to the pulse front. The beam was split into nine segments, each independently steered in space with a glass wedge to form a flat-topped intensity distribution. We measured the time-integrated laser modulation level from an equivalent target plane image of the beam. The drive pulse was a linear 1-ns ramp to about 10^{14} W/cm^2, held constant at this level for 2 ns. The shock reached the back surface of the 20-μm-thick foil at about 0.7 ns after the start of the laser pulse. The foil then accelerated at about 50 μm/ns^2, allowing for 2 ns of constant acceleration to study Rayleigh-Taylor growth. We measured the areal density modulations on the foils by conventional x-ray backlighting using a gated pinhole camera with 8-μm and 100-ps resolution [9], providing up to 12 frames per shot with arbitrary time spacing. The x-ray backlighter [10] was a uranium disk illuminated by a second 0.53-μm wavelength Nova beam (smoothed with a RPP) at about 10^{15} W/cm^2, giving a broad spectrum peaked at ~1 keV.

We have used the two-dimensional code LASNEX [11] to predict the evolution of a surface single mode for our experiment and of an imprinted single mode (produced by modulating the incident laser intensity) under the same drive conditions. The LASNEX results showed that the evolution of a laser-induced single mode parallels that of a surface single mode after the shock reaches the back surface (t_s), as is shown in Fig. 1. This suggested that the laser imprint could be calibrated to an equivalent surface finish (for our conditions). We also used the simulations to estimate the spatial amplitude (η), which corresponded to a measured modulation in optical depth ($\Delta\tau$), $\eta/\Delta\tau = 10\ \mu\text{m}/\tau$ after t_s. This allowed us to make use of the Haan [12] criterion to establish the onset of multimode nonlinear saturation. For all cases, we restricted our analysis to data that were estimated to be in the linear regime.

We analyzed each frame by converting the film density to exposure, removing the long scale length backlighter shape, filtering out noise with a parametric Wiener filter, converting to the natural logarithm of exposure (corresponding to optical depth in the foil), and finally taking the two-dimensional power spectra of the result. A typical image of ln(exposure)

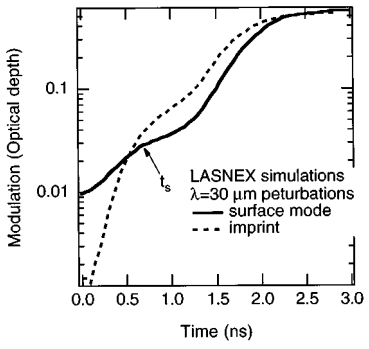

FIG. 1. LASNEX simulation of modulation of optical depth vs time for a single surface mode (solid) and a single imprinted mode (dashed) of the same wavelength (30 μm). The growth rate between t_s (0.7 ns) and the onset of saturation at $\Delta\tau = 0.3$ is 2.2 ns^{-1} for the imprinted mode and 2.5 ns^{-1} for the surface mode.

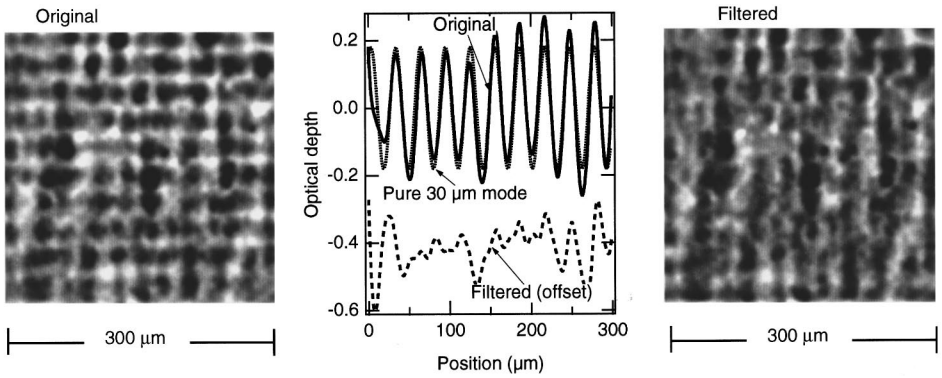

FIG. 2. A single image from a framing camera radiograph at $t=1.9$ ns (1.2 ns after t_s), shown in ln (exposure). The first image (a) has the original $\lambda=30$ μm, $\eta_0=0.25$ μm surface mode. The vertical profiles (b) are made by horizontally averaging the images. The solid curve is from (a) and the dotted curve is a pure 30-μm mode with $\eta=0.2$ (optical depth). The dashed curve corresponds to (c). Image (c) has been digitally filtered to remove the $\lambda=30$ μm mode in the vertical direction only.

is shown in Fig. 2(a), and a vertical profile that is the horizontal average of the image is shown in Fig. 2(b). The surface mode in this case was $\lambda=30$ μm (initial amplitude $\eta_0=0.25$ μm) with the modulation vector $\tilde{\mathbf{k}}$ vertical in the image, and the bandwidth was 0.9 THz. We removed the contribution of the surface mode by using a notch filter at the point in Fourier space where the surface mode appears. The same image with the surface mode thus numerically removed is shown in Fig. 2(c) and its corresponding horizontal average is the dashed line in Fig. 2(b). The radial power spectra (azimuthal integrals of the two-dimensional power spectra) for this shot at three different times, the noise power spectrum (measured on a separate shot with an undriven foil), and the instrument modulation transfer function (MTF) are shown in Figs. 3(a) and 3(b). The imprint was almost indistinguishable from the noise for the higher bandwidths at t_s (not shown), but was clearly measurable at later times. The time-integrated power spectra of the laser speckle and the imprinted spectra at $t=1.5$ ns as measured for the different bandwidths are shown in Figs. 4(a) and 4(b). As is characteristic with SSD, while there was smoothing at all modes, the higher modes were smoothed preferentially.

As a test of the LASNEX prediction that the evolution of a laser imprinted mode parallels the surface mode after t_s, we examined the growth for several shots; the results for the shot of Figs. 2 and 3 are shown in Fig. 5. The modulation amplitude for the surface mode (at $\lambda=30$ μm), for the imprinted spectrum at $\lambda=30$ μm, and for the root mean square (RMS) are shown as a function of time after the start of the laser pulse. The two $\lambda=30$ μm modes from surface and imprint modulations grow at the same rate (0.9 ± 0.2 ns^{-1}). The RMS also grows at the same rate (0.8 ± 0.2 ns^{-1}), suggesting that the growth rates for the dominant modes are similar. The values for the imprint modes have had the noise component due to the instrument and backlighter subtracted in quadrature.

The ratio of the RMS to the surface mode (at a given time in the linear regime) times the initial surface mode amplitude gave the equivalent surface finish in micrometers at $t=0$. The inferred RMS surface finish was insensitive to the calibration wavelength we used, suggesting little variation in growth rate for the dominant wavelengths. We calculated the equivalent surface finish to be 0.26 ± 0.07 μm with 0.9 THz of bandwidth on the drive laser, 0.51 ± 0.24 μm with 0.6 THz bandwidth, and 1.24 ± 0.27 μm with minimum bandwidth. These results are shown in Fig. 6 versus bandwidth, along with the time-integrated RMS modulation in the laser speckle. The imprinted modulation RMS appeared to decrease only about half as fast as the laser modulation as a function of bandwidth.

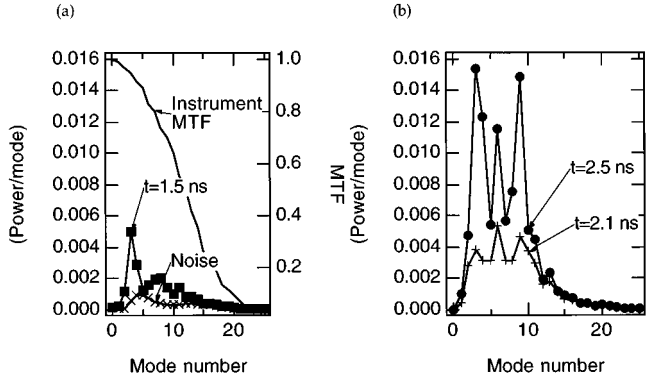

FIG. 3. Radial profiles (azimuthally integrated) at three different times of the two-dimensional Fourier power spectra for the shot shown in Fig. 2. Also shown are the instrument noise (measured on a shot with an undriven foil) and the modulation transfer function of the measurement system. The MTF uses the right-hand axis.

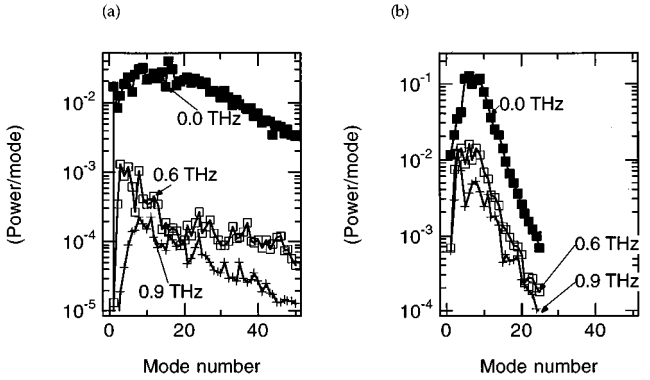

FIG. 4. Power spectra of the (a) the laser spots and (b) the imprinted modulation, converted to initial surface amplitudes, for the three bandwidths.

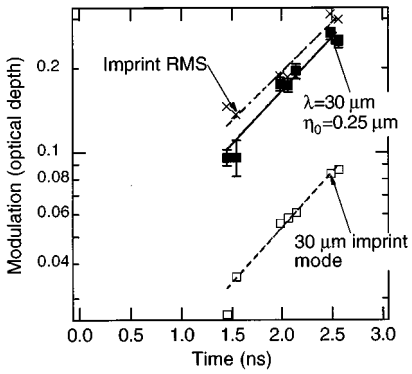

FIG. 5. Modulation amplitudes for the shot shown in Figs. 2 and 3 vs time. The surface mode (solid squares, shown with characteristic error bars), the imprinted mode at the same wavelength (open squares), and the RMS (crosses) grow at the same rate (within error bars).

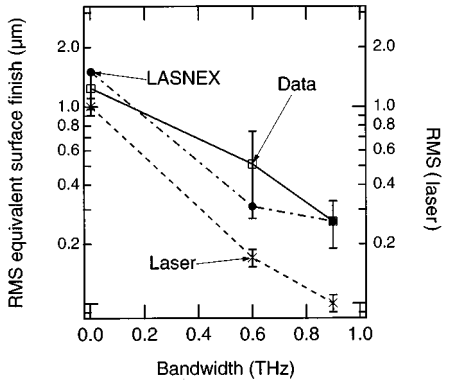

FIG. 6. Equivalent surface finish for three bandwidths, as measured (squares) and simulated (solid circles). The measured time-integrated laser RMS modulation vs bandwidth is also shown (on the right-hand axis). The lines are a guide to the eye.

We used LASNEX to simulate the equivalent surface finish due to the laser imprinted modulations. The single surface mode simulation was done separately from the laser imprint simulation. As LASNEX is a two-dimensional code, the laser speckle is represented by a one-dimensional slice of the predicted laser modulation pattern. For the case with minimum bandwidth, the speckle is isotropic and the direction of the slice is not important. When SSD was added to the simulation, we used two directions, parallel and perpendicular to the direction of dispersion, and averaged the resulting predictions. The simulations propagated the measured backlighter spectrum through the simulated package and convolved the result with the instrument response function. The results are also shown in Fig. 6. The predictions agreed with the experimental results, and also did not show as fast a decrease of imprinted modulations with bandwidth as the time-integrated laser modulation. This effect has also been observed in experiments using a different measurement technique [13,14]. One possible explanation is the thermal smoothing of the drive modulations in the region between the laser light deposition and the ablation surface. In this region, the energy is propagated by electron thermal conduction and nonuniformities are smoothed inversely with the spatial scale of the nonuniformity. The minimum-bandwidth case showed more thermal smoothing because more of the laser modulation is at smaller spatial scales. We note that if we calculate the laser time-integrated smoothing level including only lower modes (spatial structure >30 μm), the rate of decrease of target imprint and the laser time-integrated smoothing level with increased bandwidth is the same. This suggests that the thermal smoothing for this experiment is most effective for modes with wavelengths less than about 30 μm. Unfortunately, the instrument response greatly affects our ability to measure spatial structures less than 30 μm. While the LASNEX simulations predict that such structures are not present in the imprinted modulations, we cannot confirm this with the available data.

In summary, we have observed modulations due to laser speckle and we have shown that for a modest (less than a factor of 3) amount of Rayleigh-Taylor growth, the speckle imprinted modes grow at the same rate as a preimposed single mode surface perturbation. We used this to characterize the observed imprinted RMS modulation in optical depth as an equivalent surface finish for different bandwidths. The imprinted foil modulations decreased with increasing bandwidth, but not as rapidly as the time-integrated laser modulations, in agreement with numerical simulations. We suggest that the reason may be the additional smoothing of high spatial frequencies between the laser deposition region and the ablation surface.

[1] J. Nuckolls, L. Wood, A. Thiessen, and G. Zimmerman, Nature **239**, 139 (1972).
[2] M. M. Marinak *et al.*, Phys. Plasmas **3**, 2070 (1996).
[3] D. K. Bradley, J. A. Dellettrez, and C. P. Verdon, Phys. Rev. Lett. **68**, 2774 (1992).
[4] J. D. Kilkenny *et al.*, Phys. Plasmas **1**, 1379 (1994).
[5] M. H. Desselberger *et al.*, Phys. Rev. Lett. **68**, 1539 (1992).
[6] R. J. Taylor *et al.*, Phys. Rev. Lett. **76**, 1643 (1996).
[7] S. N. Dixit *et al.*, Appl. Opt. **32**, 2543 (1993).
[8] S. Skupsky *et al.*, J. Appl. Phys. **66**, 3456 (1989).
[9] O. L. Landen *et al.*, *Ultrahigh- and High-Speed Photography, Videography, and Photonics '93*, SPIE Proc. No. 2002 (SPIE, Bellingham, WA, 1993), p. 1.
[10] S. G. Glendinning *et al.*, *Applications of Laser Plasma Radiation II*, SPIE Proc. No. 2523 (SPIE, Bellingham, WA, 1995), p. 29.
[11] G. B. Zimmerman and W. L. Kruer, Comments Plasma Phys. Controlled Fusion **2**, 51 (1975).
[12] S. W. Haan, Phys. Rev. A **39**, 5812 (1989).
[13] D. H. Kalantar *et al.*, Phys. Rev. Lett. **76**, 3574 (1996).
[14] M. H. Key, *XUV Lasers and Applications*, SPIE Proc. No. 2520 (SPIE, Bellingham, WA, 1995), p. 279.